Power Research - A Journal of CPRI, Vol 22(1), 2026 | pp. 119-128

A Comparative Assessment of Steady-State Thermal Ampacity for Mixed-Voltage Cable Crossings: IEC 60287-3-3 Versus FEA-based 3D Modelling

Lijo Joseph Oliprakkattu* and Tushar Bhanudas Borole

Trident Techlabs Limited,
New Delhi – 110055, Delhi, India;
lijo.j@tridenttechlabs.com

Keywords: Ampacity, Cable Crossings, CYMCAP, IEC 60287-3-3

Article Received: 20-02-2026
Article Revised: 05-03-2026
Article Accepted: 12-03-2026

DOI: 10.33686/pwj.22.1.2026.119-128

*Author for Correspondence

Abstract

Mixed-voltage underground cable corridors frequently require crossings between high-voltage and medium-voltage circuits, where localized thermal interaction can influence allowable ampacity and long-term insulation performance. Analytical approaches for crossing assessment are widely used due to their simplicity and consistency with established current rating standards. However, the availability of finite element–based three-dimensional thermal modelling enables explicit representation of spatial heat transfer in complex installation geometries. This paper presents a comparative assessment of thermal ampacity predictions for a mixed-voltage cable crossing using an analytical method based on standard current rating formulations and a finite element–based steady-state model, both implemented in CYMCAP 9.1. Perpendicular and oblique crossing configurations are evaluated to investigate the influence of crossing angle on predicted ampacity. The study provides a structured comparison of analytical and three-dimensional modelling approaches for steady-state thermal assessment of mixed-voltage cable crossings.

This is an open access article under the terms of the CC BY: Allows others to copy, distribute, and build upon the work for any purpose, provided they credit the original creator

© 2026 The Author(s). *Central Power Research Institute* published by Informatics Publishing Limited

1. INTRODUCTION

The increasing use of underground transmission and distribution systems in urban and industrial environments has led to the frequent co-location of multiple cable circuits within constrained corridors. In such installations, crossings between high-voltage and medium-voltage cables are often unavoidable. Although the crossing region is typically limited in spatial extent, localized thermal interaction can result in elevated conductor temperatures and potential reduction in allowable ampacity. Accurate evaluation of these localized thermal effects is therefore essential to ensure reliable operation and to mitigate accelerated insulation aging and long-term cable degradation.

Steady-state current rating calculations for underground cables are commonly performed using the analytical framework defined in IEC 60287-1-1 [1]. For cable crossings involving external heat sources, IEC 60287-3-3 [2] provides a method for determining continuous current rating factors based on simplified thermal resistance networks and the principle of superposition. These analytical methods are widely adopted in engineering practice due to their computational efficiency and structured formulation. However, the analytical approach assumes uniform surrounding thermal characteristics and does not explicitly represent three-dimensional heat transfer effects that may arise in complex installation geometries.

Advancements in computational capabilities have enabled the practical application of finite element–based three-dimensional thermal modelling for underground cable systems. Such numerical models can explicitly capture radial and longitudinal heat flow, geometric interaction between crossing circuits, and localized temperature gradients in the vicinity of the crossing region.

This paper presents a comparative assessment of thermal ampacity calculations for a mixed-voltage cable crossing using the IEC 60287-3-3 analytical method and a finite element–based steady-state three-dimensional model, both implemented in CYMCAP 9.1. Perpendicular and oblique crossings are investigated to examine the influence of crossing angle on ampacity. The objective of the study is to provide a structured comparison of analytical and three-dimensional modelling approaches for steady-state thermal evaluation of underground cable crossings within a unified computational environment.

In addition to crossing angle evaluation, three-dimensional modelling provides a framework for assessing route-specific variations such as changes in burial depth, trench geometry, or proximity to adjacent infrastructure, which may introduce non-uniform thermal conditions not fully represented in simplified analytical formulations.

2. LITERATURE REVIEW

Steady-state current rating of underground power cables is commonly determined using the analytical framework defined in IEC 60287-1-1 [1], which models heat transfer through equivalent thermal resistance networks under constant load conditions. The method provides structured formulations for conductor losses, dielectric losses, sheath losses, and external thermal resistances, and remains the foundation of cable rating practice due to its simplicity and wide applicability. However, the analytical approach relies on simplified geometric assumptions and uniform thermal characteristics in the surrounding medium.

For cable crossings involving external heat sources, IEC 60287-3-3 [2] introduces a correction methodology for calculating continuous current rating factors. The approach is based on the principle of superposition and assumes uniform thermal properties around the crossing region. The analytical derivation of crossing derating equations was comprehensively developed by Anders and Brakelmann in a two-part study[3,4], where mathematical expressions for derating factors were formulated and validated through practical numerical examples. These studies demonstrated that even perpendicular crossings may lead to significant conductor temperature rise, requiring appropriate derating. Further work by Brakelmann and Anders[5] emphasized that short thermally unfavorable regions, such as localized crossings, should not be neglected despite their limited spatial extent.

While early analytical crossing formulations primarily considered radial heat transfer, later research incorporated longitudinal heat flow effects. Anders and Dorison[6] extended the analytical framework by including longitudinal heat transfer in the metallic screen, thereby improving prediction accuracy for certain crossing configurations. Similarly, Zheng *et al.*[7] developed a three-dimensional heat network model derived from Fourier's law and energy balance equations, incorporating both radial and longitudinal heat flow. Their results highlighted the importance of longitudinal temperature gradients in pipe-type cable crossings and demonstrated measurable ampacity reduction under unfavorable thermal conditions.

Advancements in computational methods have enabled the broader application of finite element analysis to cable rating problems. Dubitsky *et al.*[8] presented a systematic comparison between IEC 60287 calculations and finite element simulations, showing close agreement for simple cable arrangements but identifying stronger thermal interaction effects in more complex layouts. Three-dimensional modelling techniques allow explicit representation of geometric interaction and localized heat diffusion beyond the simplified resistance-network approach. Zairis *et al.*[9] demonstrated that three-dimensional finite element modelling is necessary for accurately evaluating complex cable crossings, particularly where longitudinal heat conduction and non-uniform geometry are present. More recently, Brakelmann and Anders[10] proposed an advanced analytical formulation for complex cable arrangements, bridging traditional analytical methods and full numerical simulations.

Beyond single crossing configurations, multiple crossing interactions have also been investigated. Radzi *et al.*[11] analyzed multiple high-voltage and medium-voltage cable crossings using numerical modelling and showed that neglecting localized thermal interaction may result in unacceptable conductor temperatures and accelerated insulation aging. These studies collectively indicate that crossing geometry, installation configuration, and thermal interaction effects can significantly influence predicted ampacity.

Although previous studies have developed analytical derating equations, incorporated longitudinal heat flow effects, and applied finite element modelling to complex cable arrangements, few investigations have performed a controlled validation of IEC 60287-3-3 analytical predictions against finite element–based three-dimensional modelling under identical installation and boundary conditions. In particular, comparative assessments conducted within a unified computational environment for mixed-voltage cable crossings remain limited. Furthermore, the influence of crossing angle on the consistency between analytical and numerical steady-state predictions has not been systematically evaluated under consistent modelling assumptions.

The present study addresses this gap by performing a comparative assessment of IEC 60287-3-3 analytical calculations and finite element–based steady-state three-dimensional modelling implemented in CYMCAP 9.1. Perpendicular and oblique crossing configurations are evaluated under identical soil and boundary conditions to examine the relative consistency and applicability of analytical and three-dimensional approaches for steady-state thermal assessment of underground cable crossings.

3. SYSTEM CONFIGURATION

This section describes the cable configurations, installation geometry, and thermal boundary conditions considered in the comparative assessment. A mixed-voltage crossing between a high-voltage transmission cable and a sub-transmission cable is modelled under steady-state conditions. Installation parameters were kept consistent for both approaches to ensure controlled comparison.

3.1 Cable Description

The high-voltage circuit consists of a 132 kV single-core cable corresponding to the CIGRE 1A reference design with a conductor cross-sectional area of 1200 mm². The sub-transmission circuit consists of a 33 kV single-core cable corresponding to the CIGRE 4A reference design with a conductor cross-sectional area of 240 mm².

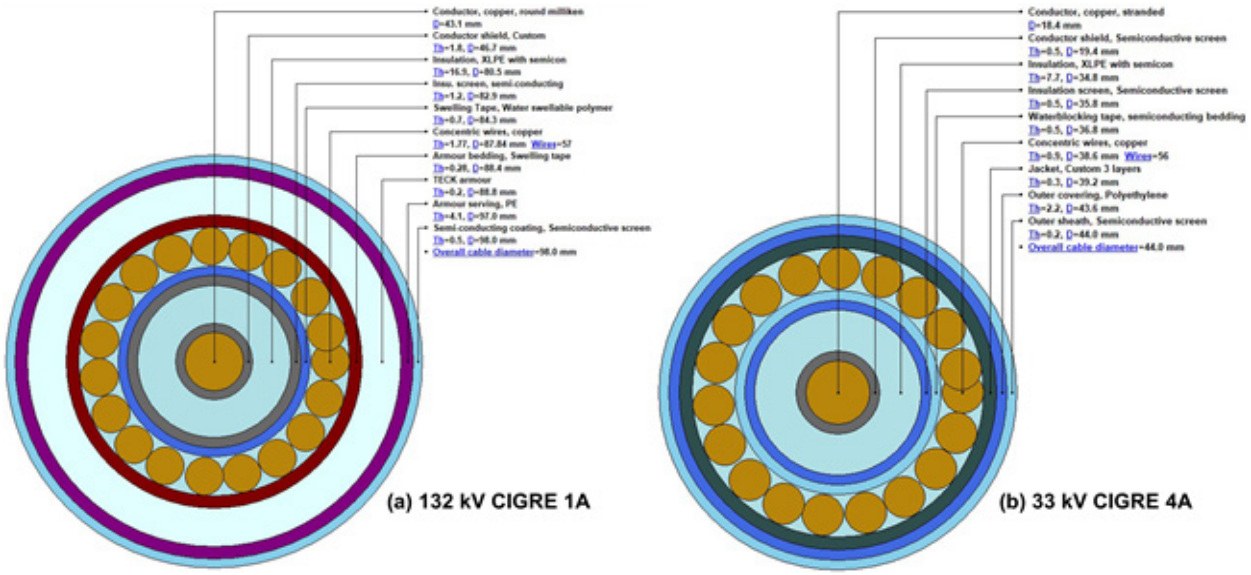


Figure 1. Cable cross-sections used in the study: **(a)** 132 kV CIGRE 1A, **(b)** 33 kV CIGRE 4A, modelled in CYMCAP 9.1.

Both cables were defined in CYMCAP 9.1 [12] using the standard geometric and material parameters associated with the respective CIGRE configurations. The cross-sectional constructions of the cables as modelled in CYMCAP are shown in Figure 1 and Figure 2.

Figure 1. both circuits are arranged in trefoil formation and operate at a frequency of 50 Hz. The metallic sheaths are cross-bonded with equal minor section lengths assumed for steady-state evaluation. The maximum allowable conductor temperature for both circuits is limited to 90°C.

Installation Geometry

The installation geometry consists of a mixed-voltage crossing between a 132 kV transmission cable and a 33 kV sub-transmission cable. The crossing occurs

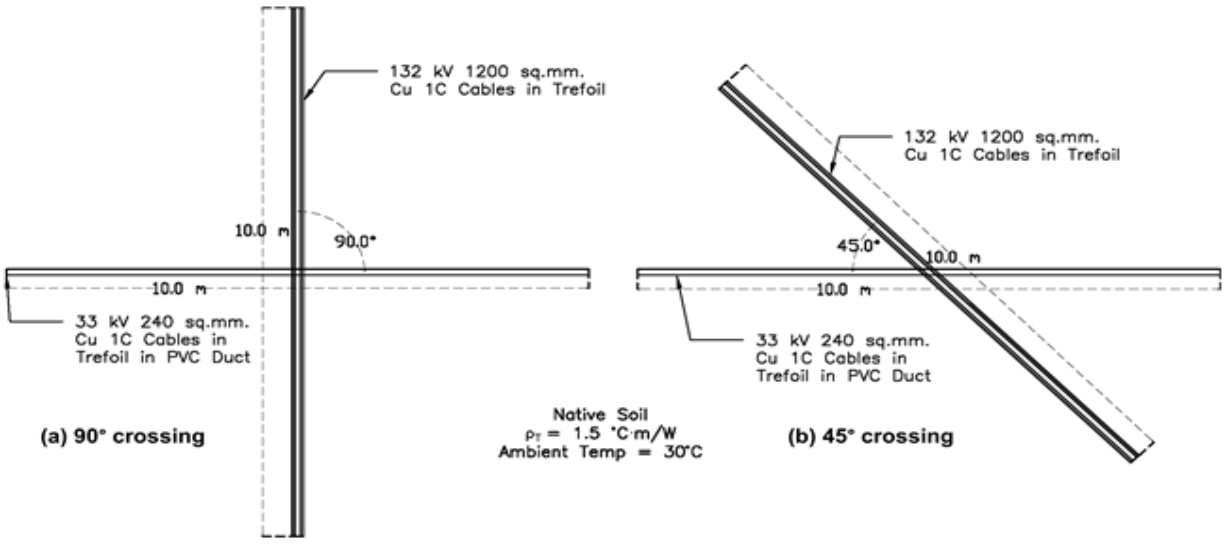


Figure 2. Plan view of crossing configurations considered in the study: **(a)** 90° crossing, **(b)** 45° crossing.

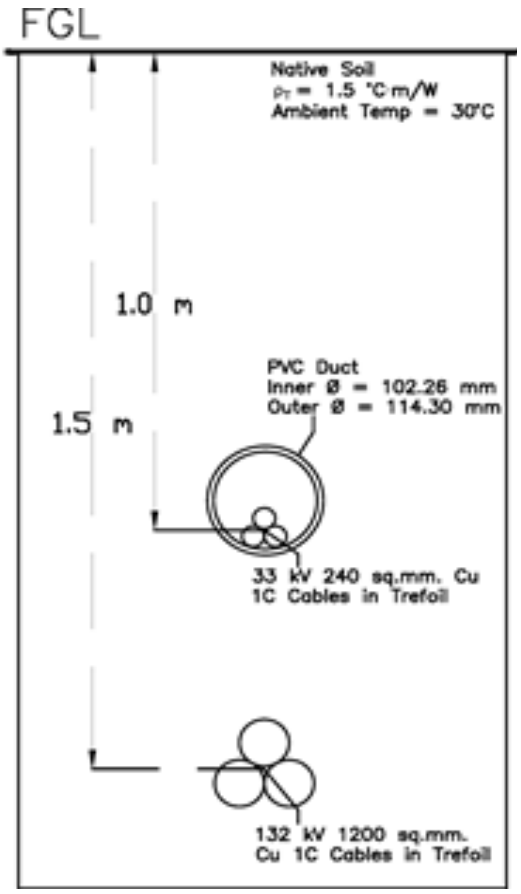


Figure 3. Trench section showing burial depths of the 33 kV cable (in PVC duct) and the 132 kV direct-buried cable.

at the geometric mid-point of both cable sections. Two crossing configurations are investigated: A perpendicular (90°) crossing and an oblique (45°) crossing. The corresponding plan views illustrating the crossing orientations are shown in Figure 2.

The 33 kV circuit is installed at a burial depth of 1.0 m, measured from ground surface to cable centerline, and is placed inside a PVC duct assumed to be air-filled for steady-state thermal modelling. The 132 kV circuit is directly buried at a depth of 1.5 m to cable centerline. The trench section illustrating the relative burial depths is shown in Figure 3.

3.2 Thermal and Boundary Conditions

The thermal environment is assumed to be homogeneous and isotropic. The surrounding soil is modelled with a thermal resistivity of 1.5 °C·m/W. The ambient soil temperature is taken as 30°C. Steady-state operating conditions are assumed, corresponding to a continuous constant current sufficient to produce asymptotic maximum conductor temperature under uniform environmental conditions.

The PVC duct surrounding the 33 kV cable is assumed to be air-filled, and no forced cooling or additional thermal enhancement materials are considered. Both circuits are evaluated with a maximum allowable conductor temperature of 90°C.

For comparative consistency, identical thermal properties, burial depths, and environmental conditions are applied to both the analytical and the three-dimensional modelling approaches. This ensures that any differences in predicted ampacity arise from methodological formulation rather than variation in installation parameters.

4. METHODOLOGY

The comparative assessment presented in this study is based on two steady-state thermal evaluation approaches: an analytical crossing method derived from IEC 60287-3-3 [2] and a finite element–based three-dimensional thermal model. Both approaches were implemented in CYMCAP 9.1 [12] under identical conditions to ensure consistency.

4.1 Analytical Crossing Method

The analytical evaluation of the cable crossing is based on the methodology described in IEC 60287-3-3 [2]. The standard provides a procedure for calculating the continuous current rating factor for cables crossing external heat sources. The formulation relies on the principle of superposition and assumes uniform thermal properties in the surrounding soil.

In this study, the crossing module implementing IEC 60287-3-3 was used to determine the allowable ampacity of both circuits under steady-state conditions. The method computes derating factors by modifying the thermal resistance network to account for the localized heat source effect at the crossing region.

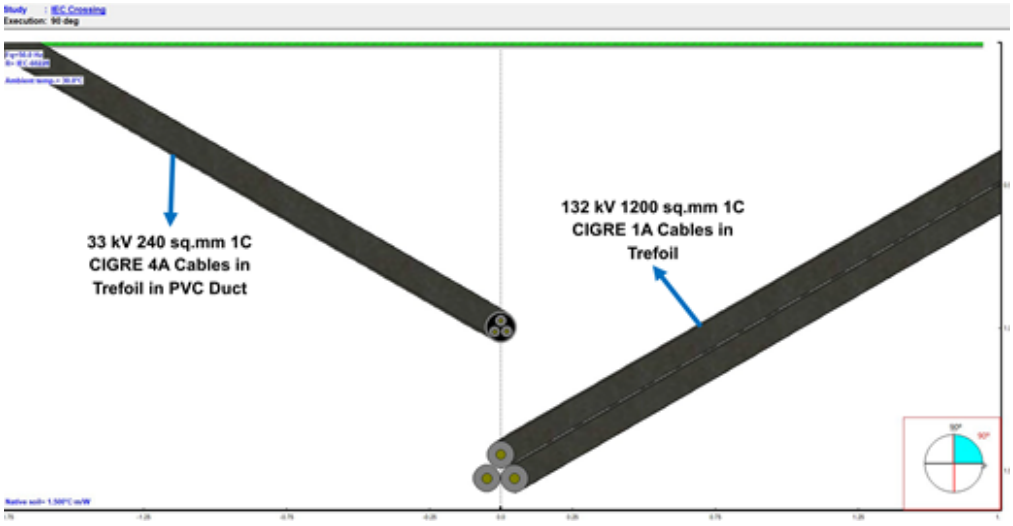


Figure 4. Implementation of the IEC 60287-3-3 crossing calculation in CYMCAP 9.1 (90° configuration).

The conductor temperature is assumed to be limited to 90°C, and the permissible currents are calculated accordingly.

The analytical method inherently assumes simplified spatial heat flow representation and does not explicitly model longitudinal heat transfer effects beyond the equivalent resistance formulation.

The implementation of the analytical crossing calculation in CYMCAP 9.1 is illustrated in Figure 4.

The same procedure was repeated for the 45° crossing configuration by modifying the crossing angle parameter while maintaining identical installation conditions.

4.2 Finite Element–Based Three-Dimensional Modelling

The three-dimensional approach employs a steady-state thermal model based on finite element analysis.

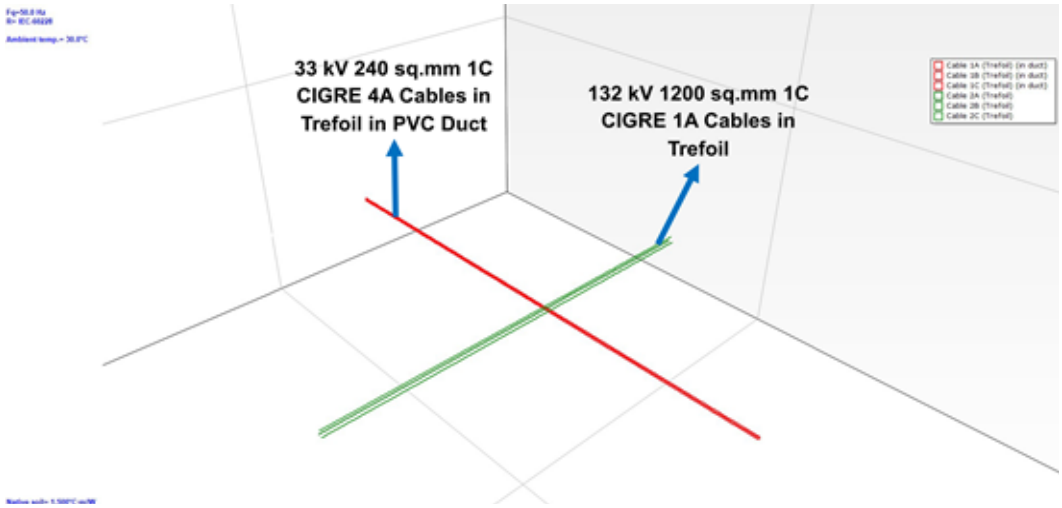


Figure 5. Three-dimensional representation of the cable crossing model in CYMCAP 9.1 (90° configuration).

The physical geometry described in Section 3 was reproduced in three-dimensional space, with each cable section defined over a total length of 10 m. The crossing was positioned at the geometric mid-point of both cable sections to allow symmetric longitudinal heat distribution.

The three-dimensional model representation in CYMCAP 9.1 is shown in Figure 5.

The model explicitly captures radial and longitudinal heat transfer within the conductors, insulation layers, metallic sheaths, duct region, and surrounding soil. Uniform soil thermal resistivity and ambient temperature were applied as boundary conditions.

For comparative consistency, the 33 kV circuit current was fixed at 315 A for both crossing angles. The 132 kV circuit current was iteratively adjusted until the conductor temperature reached the limiting value of 90°C. This iterative approach ensured that the maximum allowable conductor temperature was achieved under steady-state conditions for each crossing configuration.

4.3 Comparative Framework

To ensure a structured comparison, identical installation geometry, soil properties, burial depths, and temperature limits were applied in both analytical and three-dimensional approaches. The comparison focuses on the maximum allowable steady-state current for each circuit under 90° and 45° crossing conditions.

Differences in predicted ampacity are therefore attributable to methodological formulation, including the analytical superposition assumption in IEC 60287-3-3 [2] and the explicit spatial heat transfer modelling in the finite element approach.

5. RESULTS

The steady-state ampacity results obtained from the analytical crossing method and the three-dimensional thermal model are presented for both 90° and 45° crossing configurations. For consistency, the 33 kV circuit current was fixed at 315 A in the three-dimensional model, and the 132 kV current was iteratively adjusted to reach the conductor temperature limit of 90°C.

5.1 90° Crossing Configuration

The results for the perpendicular (90°) crossing are summarized in Table 1.

Table 1. Comparison of analytical and three-dimensional results for 90° crossing configuration

Method	132 kV Current (A)	132 kV Max Cond Temp (°C)	33 kV Current (A)	33 kV Max Cond Temp (°C)
IEC 60287-3-3	849.5	90.0	328.8	90.0
3D Model	814.9	90.0	315.0	89.54

For the 90° crossing, the analytical method predicts a higher allowable current for the 132 kV circuit compared to the three-dimensional model.

5.2 45° Crossing Configuration

The results for the oblique (45°) crossing are summarized in Table 2.

Table 2. Comparison of analytical and three-dimensional results for 45° crossing configuration

Method	132 kV Current (A)	132 kV Max Cond Temp (°C)	33 kV Current (A)	33 kV Max Cond Temp (°C)
IEC 60287-3-3	842.1	90.0	324.5	90.0
3D Model	813.9	90.0	315.0	89.61

For the 45° crossing, a similar trend is observed. The analytical method yields slightly higher allowable current compared to the three-dimensional model. The temperature of the 33 kV circuit remains below the

maximum allowable value in the three-dimensional analysis due to the fixed current condition.

5.3 Comparative Observation

Table 3. Summary comparison of calculated 132 kV ampacity for analytical and three-dimensional approaches

Crossing Angle	IEC 60287-3-3 (A)	3D Model (A)	Deviation (%)
90°	849.5	814.9	+4.3
45°	842.1	813.9	+3.5

As summarized in Table 3, the analytical method predicts higher allowable current for the 132 kV circuit, with deviation within approximately 3-4%.

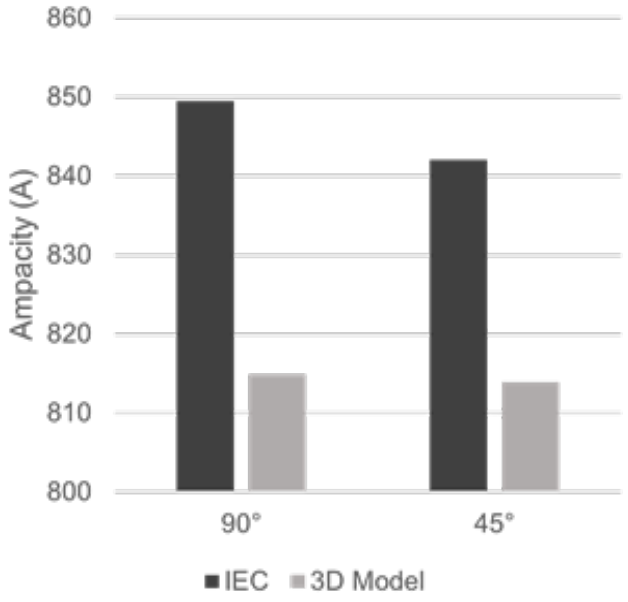


Figure 6. Comparison of calculated 132 kV ampacity for analytical and three-dimensional approaches under 90° and 45° crossing configurations.

A reduction in allowable current is observed when transitioning from the 90° to the 45° crossing in both analytical and three-dimensional approaches, indicating sensitivity to crossing geometry. The deviation between the two methodologies remains moderate and systematic, with the analytical approach consistently yielding higher ampacity values.

6. COMPARATIVE ANALYSIS

The results presented in Section 5 indicate that the analytical crossing method based on IEC 60287-3-3 [2] consistently predicts higher allowable currents for the 132 kV circuit compared to the three-dimensional thermal model. This trend is observed for both the 90° and 45° crossing configurations.

The IEC analytical formulation is based on an equivalent thermal resistance network and the principle of superposition [2]. In this representation, the thermal interaction between crossing circuits is incorporated through modified equivalent resistance terms that approximate the mutual heating effect. However, the method does not explicitly resolve localized spatial temperature gradients along the cable axis. Instead, the crossing interaction is effectively distributed over an averaged thermal path within the resistance network.

In contrast, the three-dimensional model directly resolves the finite spatial extent of the crossing region and captures localized temperature peaks that arise due to concentrated mutual heating. Explicit representation of longitudinal heat conduction and finite cable length effects produces a localized temperature distribution influencing the current required to reach the 90°C limit. This difference in spatial heat representation contributes to the slightly lower ampacity predicted by the three-dimensional model.

A reduction in allowable current is observed when transitioning from the perpendicular (90°) to the oblique (45°) crossing configuration in both methodologies. The oblique crossing increases the effective thermal interaction length between the circuits, resulting in greater mutual heating influence and corresponding ampacity reduction. The consistency of this trend across both analytical and three-dimensional approaches confirms the physical validity of the modelling assumptions.

The deviation between the two methods remains moderate and systematic. The analytical approach provides a conservative and standardized evaluation framework suitable for practical design assessments, while the three-dimensional model offers enhanced

spatial resolution and improved representation of localized thermal interaction. Both approaches produce comparable trends, with differences attributable to modelling formulation.

Beyond crossing angle effects, three-dimensional modelling becomes valuable when installation parameters vary along the route. Changes in burial depth, trench geometry, duct configuration, or proximity to other thermal influences introduce non-uniform boundary conditions not readily represented by equivalent thermal resistance formulations. Such variations may affect conductor temperature beyond the immediate crossing region. Finite element–based three-dimensional modelling enables explicit representation of these geometric and environmental effects, supporting assessment of route-specific thermal behavior not captured through analytical superposition. This capability is particularly relevant in constrained urban corridors requiring depth variation or proximity to infrastructure.

7. CONCLUSION

This paper presented a comparative assessment of steady-state thermal ampacity for a mixed-voltage cable crossing using the IEC 60287-3-3 analytical method and a finite element–based three-dimensional model implemented in CYMCAP. Both perpendicular and oblique configurations were evaluated under identical conditions.

The analytical method consistently predicted slightly higher allowable current for the 132 kV circuit, with deviation remaining within approximately 3-4% relative to the three-dimensional model. The difference arises from the simplified equivalent thermal resistance formulation in the analytical approach, whereas the three-dimensional model resolves localized spatial heat transfer, including longitudinal conduction.

Both methods demonstrated consistent sensitivity to crossing angle, confirming increased thermal interaction for oblique configurations. While analytical calculations remain suitable for routine assessments, three-dimensional modelling in CYMCAP provides confidence for high-capacity circuits near thermal limits.

8. ACKNOWLEDGMENT

The authors acknowledge the financial and organizational support provided by Trident Techlabs Limited for the preparation and presentation of this paper.

9. REFERENCES

1. International Electrotechnical Commission. IEC 60287-1-1:2023 Electric cables - Calculation of the current rating - Part 1-1: Current rating equations (100% load factor) and calculation of losses - General. Geneva: International Electrotechnical Commission; 2023.
2. International Electrotechnical Commission. IEC 60287-3-3:2007 Electric cables - Calculation of the current rating - Part 3-3: Sections on operating conditions - Cables crossing external heat sources. Geneva: International Electrotechnical Commission; 2007.
3. Anders G, Brakelmann H. Cable crossings: derating considerations. I. Derivation of derating equations. IEEE Trans Power Deliv. 1999; 14(3):709-714. https://doi.org/10.1109/61.772304
4. Anders G, Brakelmann H. Cable crossings: derating considerations. II. Example of derivation of derating curves. IEEE Trans Power Deliv. 1999; 14(3):715-720. https://doi.org/10.1109/61.772305
5. Brakelmann H, Anders G. Ampacity reduction factors for cables crossing thermally unfavorable regions. IEEE Trans Power Deliv. 2001; 16(4):444-448. https://doi.org/10.1109/61.956718
6. Anders GJ, Dorison E. Derating factor for cable crossings with consideration of longitudinal heat flow in cable screen. IEEE Trans Power Deliv. 2004; 19(3):926-932. https://doi.org/10.1109/TPWRD.2003.822961
7. Zheng YL, Xu ZL, Zhang GJ. Analysis on the longitudinal temperature and computation of ampacity of 10 kV cables in pipes crossing unfavorable thermal regions. In: Proceedings of the IEEE International Conference on the Properties and Applications of Dielectric Materials; 2012; Bangalore, India. https://doi.org/10.1109/ICPADM.2012.6319002

8. Dubitsky S, Greshnyakov G, Korovkin N. Comparison of finite element analysis to IEC-60287 for predicting underground cable ampacity. In: Proceedings of the IEEE International Energy Conference (ENERGYCON); 2016; Leuven, Belgium. https://doi.org/10.1109/ENERGYCON.2016.7514107

9. Zairis P, Chatzipetros D, Liangou T, Bitsi K, Chrysochos AI. 3D thermal analysis of complex cable crossings. In: COMSOL Conference 2024; 2024; Florence, Italy.

10. Brakelmann H, Anders GJ. A new method for analyzing complex cable arrangements. IEEE Trans Power Deliv. 2022; 37(3):1608-1616. https://doi.org/10.1109/TPWRD.2021.3094666

11. Radzi AS, Nor Arifin NA, Anthony TM, Aida Z, Azlina N, Raj A, Chakrabarty C, Syaza N. The effect on ampacity for multiple cable crossing and mitigation to improve its ampacity. In: Proceedings of the IEEE International Conference on Power and Energy (PECon); 2016; Melaka, Malaysia. https://doi.org/10.1109/PECON.2016.7951577

12. CYME International T&D. CYMCAP 9.0 - Reference Manual. Montreal (QC): CYME International T&D; 2024.